

Supporting Information

Polymer brush based fluorescent immunosensing device on stainless steel for spatially localized detection of interleukin-1 β in rat blood

Fei Deng^{a, b}, Yi Li,^{a, b} Md Jakir Hossain^c, Michael D Kendig^c, Ria Arnold^c, Ewa M. Goldys^{a, b},

Margaret J. Morris^c, Guozhen Liu^{* a, b}

^aGraduate School of Biomedical Engineering, ARC Centre of Excellence in Nanoscale

Biophotonics, Faculty of Engineering, UNSW Sydney, NSW 2052, Australia

^bAustralian Centre for NanoMedicine, UNSW Sydney, NSW 2052, Australia

^cSchool of Medical Sciences, UNSW Sydney, NSW 2052, Australia

*Corresponding Author: Dr. Guozhen Liu, email: guozhen.liu@unsw.edu.au Tel: +61-2-9385 0714

1. Protocols for fabrication of the stainless steel immunosensor

The sensing interface was fabricated in a step-wise fashion. Firstly, SS ribbons with the length of 1 cm were rinsed with copious amount of deionized water, acetone, ethanol and deionized water, respectively, to degrease and clean the surface. Then clean SS ribbons were activated by immersion into the piranha solution ($\text{H}_2\text{SO}_4:\text{H}_2\text{O}_2 = 3:1$, v/v) for 30 min to generate a hydroxyl-enriched surface. After the reaction, the SS ribbons were rinsed with deionized water and dried under nitrogen stream before being immersed in a 1 mg mL⁻¹ aqueous solution of dopamine (pH=11) for 24 h. The substrates were then rinsed with copious amount of deionized water to remove the unreacted dopamine monomer to achieve the SS-PDA surface. The immobilization of the alkyl bromine ATRP initiator on SS-PDA substrates

was conducted in anhydrous CH_2Cl_2 solution (10 mL) with the help of TEA (0.5 mL) and BIBB (0.45 mL) under argon atmosphere for 2 h in ice bath. The resulting SS-Br substrates were rinsed with deionized water and stored under nitrogen atmosphere.

The grafting of PEGMA brushes on SS-Br surface was carried out using PEGMA, CuBr, CuBr_2 and bpy (molar ratio, 100:1:0.2:2) in methanol/water (1:1, v:v) solution at 35 °C for 4 h. Firstly, 38.36 mg of the ligand bpy was placed in a clean flask and dissolved using 10 mL of 1:1 methanol/water (v/v) mixture at 35 °C under argon atmosphere. Next, 5.5 mg of CuBr_2 was added into the solution and allowed to dissolve. Thereafter PEGMA (4 mL) was added to the solution with stirring under argon flow for 10 min before the addition of 17.68 mg of the activator CuBr, which could dissolve under argon flow. After gently purging with argon for 10 min, the SS-Br was immersed in the solution for 4 h to achieve the polymer brush surface (SS-PEGMA), which was washed with ethanol and deionized water, and dried under nitrogen stream before the next step of treatment. In order to have the densely packed polymer brush, the above process could be repeated to get SS-PEGMA II and SS-PEGMA III.

Before immobilization of IL-1 β polyclonal antibody on the substrate surfaces, the SS-PEGMA substrates were immersed in 1 mL of dried DMSO, containing 0.04 g CDI and 0.04 g DMAP for 24 h at room temperature to give rise to the SS-PEGMA-CDI surfaces. Then the substrates were rinsed with copious amounts of THF and deionized water before incubation in 0.1 mL PBS solution containing 2 $\mu\text{g mL}^{-1}$ IL-1 β polyclonal antibody. The immobilization reaction could proceed at 4 °C for 24 h to produce the SS-PEGMA-Abs sensing interfaces, which were rinsed with PBS solution and deionized water before usage.

2. Protocol for characterization of stainless steel device

The attenuated total reflectance-Fourier transform infrared spectra (ATR-FTIR) was measured on a Nicolet FTIR Spectrometer. The reported spectra were the accumulated average of 32 scans at 4 cm⁻¹ resolution from 500 to 4000 cm⁻¹.

Static water contact angles of various substrate surfaces were measured at 25 °C and 60% relative humidity with 5 μL water droplet by Drop Shape Analyzer-DSA30. The contact angles reported were the mean values of ten tests from different surface locations.

3. Optimization of the polymer brush modified SS surfaces

The successfully synthesized SS-PEGMA polymer brushes were characterized by ATR-FTIR. As shown in Figure S1, the aromatic peak of SS-PDA indicated successful coating of PDA on SS. And the C=O peak in SS-PEGMA demonstrated the successful grafted PEGMA brushes on the surface of SS-PDA.

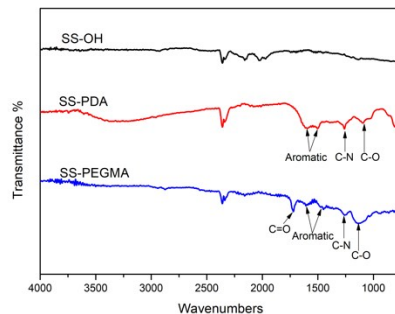


Figure S1. ATR-FTIR figures of SS, SS-PDA and SS-PEGMA.

The strong light signals from SS were eliminated by three approaches (Figure S2), including replacement of substrate, surface coating of substrate and usage of special fluorophores. Figure S2a shows results of the replacement of substrate where both copper and platinum show strong light signals. Figure S2b shows that after surface coating, both SS-PDA and SS-PEGMA continue showing light signals. We then explored selected fluorophores applied on SS as shown in Figure S2c, to verify if their signal is able to overcome the SS background. FITC showed

very weak fluorescence contrast. However, the contrast for NBD was improved, and PE and NR beads showed high contrast.

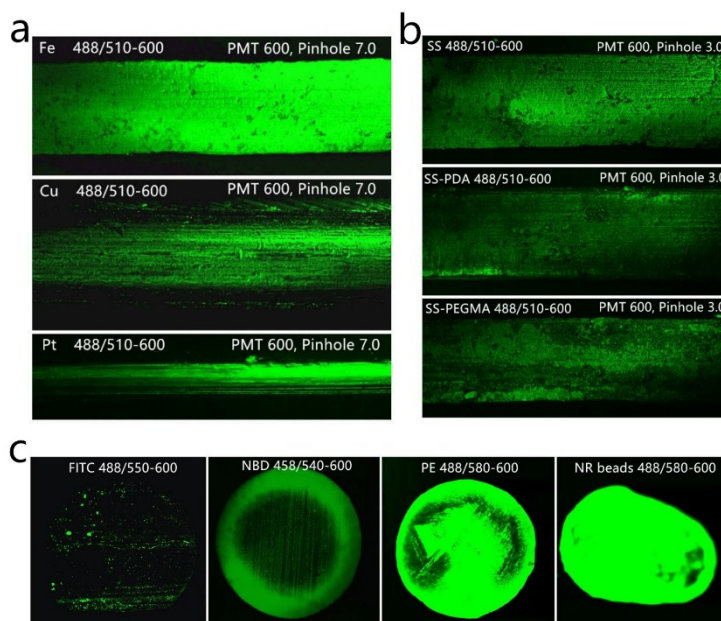


Figure S2. (a) The scattering of different metals; (b) the scattering of SS, SS-PDA, SS-PEGMA; (c) different fluorophores on SS (PMT:600 volts, pinhole: 3.0, concentration: 100 $\mu\text{g mL}^{-1}$).

The calibration curve of the fluorescence intensity versus the concentration of secondary antibody is shown in Figure S3; the fluorescence intensity linearly increased with the secondary antibody concentration, and the linear regression equation was $y=9.43 \times 10^6 c + 919295$ with a correlation coefficient of 0.995.

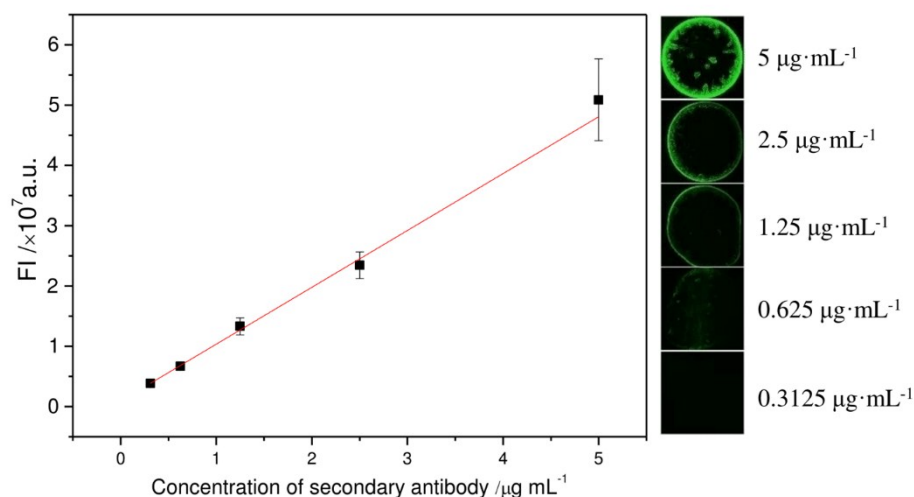


Figure S3. The calibration curve of the fluorescence intensity versus the concentration of secondary antibody.

In order to study the influence of the length and density of PEGMA polymer brushes, SS-PEGMA I, SS-PEGMA II and SS-PEGMA III were produced.¹ As shown in Figure S4a, with the increase of repeating times, the fluorescence intensity of SS sensing interface decreased. The possible reason was due to the instability of polymer brushes, whereby the high graft density manifests as a large entropic force due to chain stretching (mechanical instability) strong enough to weaken the metal-organic interface. Therefore, SS-PEGMA was used in our current research.

The incubation time of the antibody-antigen binding in this immunoassay was also investigated. The SS device was incubated in 200 pg mL^{-1} IL-1 β solution with different incubation times. As shown in Figure S4b, the fluorescence intensity increased significantly with the increased incubation time from 0 to 120 min and then slightly changed after two hours, indicating that the binding reaction was nearly finished at that time. Compared with our previous research for the detection of IL-6 (200 pg mL^{-1}), the best incubation time of Liu et al's optical fibre test strip² was 30 min, and the best incubation time of Zhang et al's optical fibre immunosensor³ was 60 min. The possible reason for the difference of incubation time for

IL-6 was due to the difference of immunosensing system. However, in our present research, the best incubation time was 120 min; the possible reason was due to the antifouling properties of PEGMA polymer brushes, which slowed down the antibody-antigen binding reaction. The fluorescence intensity in 30 min was about half of the fluorescence intensity in 120 min, indicating that 30 min is also suitable for the detection of IL-1 β . If lower cytokine concentration was applied, the best incubation time would be shorter. In Zhang et al's optical fibre immunosensor⁴ for the detection of IL-6, the best incubation time was 30 min when the concentration of IL-6 was 5 pg mL⁻¹. In addition, Zhang et al's optical fibre immunosensor³ for the detection of IL-1 β , showed a best incubation time of 30 min when the concentration of IL-1 β was 10 pg mL⁻¹. Therefore, the sensor system and cytokine concentration will both influence the incubation time.

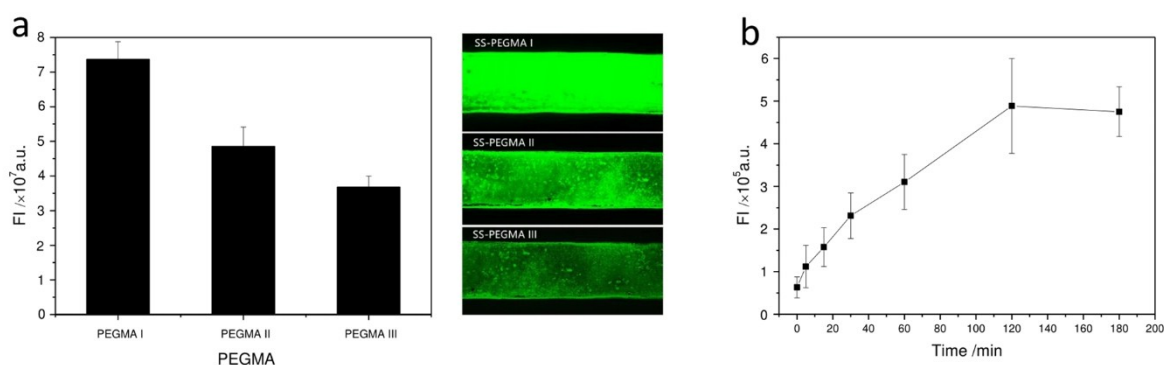


Figure S4. (a) The fluorescence intensity of SS immunosensor with different length of PEGMA brushes; (b) the optimization of SS immunosensor's incubation time.

4. Bland-Altman Plot between herein fabricated assay with ELISA

The Bland-Altman Plot of cell experiment is shown in Figure S5. The difference between two measurements were all located in the 95% limits of agreement, indicating the two methods could be used interchangeably.

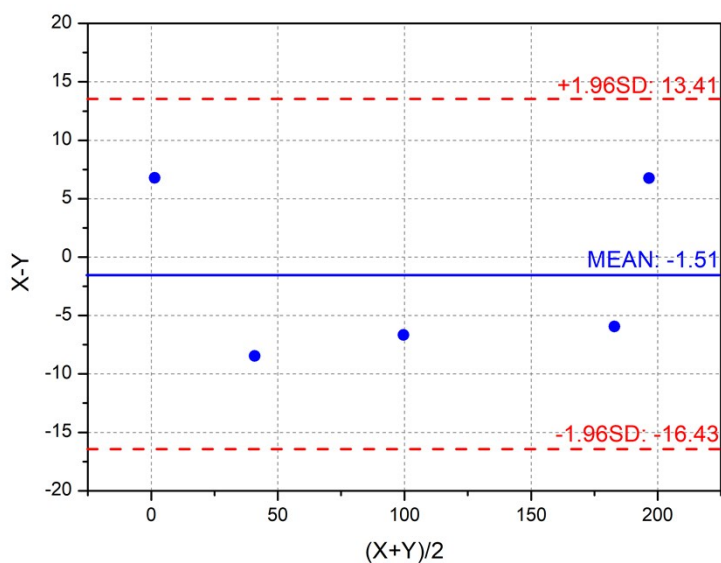


Figure S5. The Bland-Altman Plot of cell experiment.

5. Real photo of SS ribbon

This is the real photo of SS ribbon, which was got by microscope, and the width of SS ribbon is 0.5 mm.

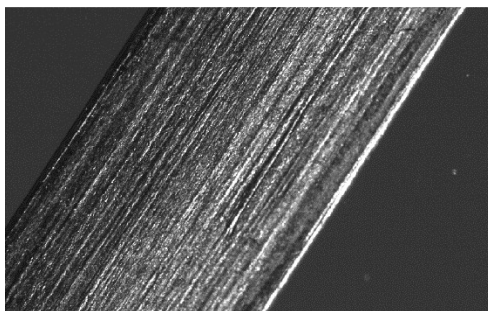


Figure S6. The microscopy image of SS ribbon.

6. Comparison of the analytical performances of herein immunosensor with other recently reported sensors for IL-1 β detection

Table S1. Comparison of the analytical performances of herein immunosensor with other recently reported sensors for IL-1 β detection.

Sensors	Linear range (pg mL ⁻¹)	Detection limit (pg mL ⁻¹)	Sample types	Minimum sample volume (μL)	Year	Reference
ELISA kit	31.3-2000	5	Cell culture supernates, serum, EDTA plasma	50	2019	R&D
Optical fibre based biosensor	3.13-400	1.12	Rat spine cord	NA	2019	[1]
Impedimetric immunosensor	0.01-3	0.001	Serum and saliva	NA	2018	[2]
Optical fibre based biosensor	3.9-500	1.2	hippocampus	NA	2018	[3]
Electrochemical immunosensor	0.5-100	0.38	Serum	2.5	2017	[4]
Impedimetric immunosensor	1-15	NA	NO	NA	2017	[5]
Amperometric microfluidic array	50-500	0.01	Serum	5	2015	[6]
Dendrimer-based assay	0.98-250	1.15	No	100	2010	[7]
Microarray technology	11.7-175	11.7	No	No	2010	[8]
Plasmon resonance sensor	50-10000	21	Synovial fluids	200	2010	[9]
Surface plasmon resonance sensor	10 ³ -10 ⁵	290	Cell culture medium	NA	2005	[10]
SS based biosensor here	12.5-200	4.7	Plasma, whole blood	1	NA	This work

References

1. Friis, J. E.; Brons, K.; Salmi, Z.; Shimizu, K.; Subbiahdoss, G.; Holm, A. H.; Santos, O.; Pedersen, S. U.; Meyer, R. L.; Daasbjerg, K.; Iruthayaraj, J., Hydrophilic Polymer Brush Layers on Stainless Steel Using Multilayered ATRP Initiator Layer. *ACS Appl Mater Interfaces* **2016**, *8* (44), 30616-30627.

2. Liu, G.; Zhang, K.; Nadort, A.; Hutchinson, M. R.; Goldys, E. M., Sensitive Cytokine Assay Based on Optical Fiber Allowing Localized and Spatially Resolved Detection of Interleukin-6. *ACS Sens* **2017**, 2 (2), 218-226.
3. Zhang, K.; Baratta, M. V.; Liu, G.; Frank, M. G.; Leslie, N. R.; Watkins, L. R.; Maier, S. F.; Hutchinson, M. R.; Goldys, E. M., A novel platform for in vivo detection of cytokine release within discrete brain regions. *Brain Behav Immun* **2018**, 71, 18-22.
4. Zhang, K.; Liu, G.; Goldys, E. M., Robust immunosensing system based on biotin-streptavidin coupling for spatially localized femtogram mL(-1) level detection of interleukin-6. *Biosens Bioelectron* **2018**, 102, 80-86.
5. Zhang, K.; Arman, A.; Anwer, A. G.; Hutchinson, M. R.; Goldys, E. M., An optical fiber based immunosensor for localized detection of IL-1 β in rat spinal cord. *Sensors and Actuators B: Chemical* **2019**, 282, 122-129.
6. Aydın, E. B.; Aydın, M.; Sezgintürk, M. K., Highly sensitive electrochemical immunosensor based on polythiophene polymer with densely populated carboxyl groups as immobilization matrix for detection of interleukin 1 β in human serum and saliva. *Sensors and Actuators B: Chemical* **2018**, 270, 18-27.
7. Sanchez-Tirado, E.; Salvo, C.; Gonzalez-Cortes, A.; Yanez-Sedeno, P.; Langa, F.; Pingarron, J. M., Electrochemical immunosensor for simultaneous determination of interleukin-1 beta and tumor necrosis factor alpha in serum and saliva using dual screen printed electrodes modified with functionalized double-walled carbon nanotubes. *Anal Chim Acta* **2017**, 959, 66-73.
8. Baraket, A.; Lee, M.; Zine, N.; Sigaud, M.; Bausells, J.; Errachid, A., A fully integrated electrochemical biosensor platform fabrication process for cytokines detection. *Biosens Bioelectron* **2017**, 93, 170-175.

9. Krause, C. E.; Otieno, B. A.; Bishop, G. W.; Phadke, G.; Choquette, L.; Lalla, R. V.; Peterson, D. E.; Rusling, J. F., Ultrasensitive microfluidic array for serum pro-inflammatory cytokines and C-reactive protein to assess oral mucositis risk in cancer patients. *Anal Bioanal Chem* **2015**, *407* (23), 7239-43.
10. Han, H. J.; Kannan, R. M.; Wang, S.; Mao, G.; Kusanovic, J. P.; Romero, R., Multifunctional Dendrimer-templated Antibody Presentation on Biosensor Surfaces for Improved Biomarker Detection. *Adv Funct Mater* **2010**, *20* (3), 409-421.
11. Reuven Duer, R. L., Richard Tanaka, Douglas A. Christensen, James N. Herron, In-plane parallel scanning: A microarray technology for point-of-care testing. *Anal. Chem.* **2010**, *82*, 8856-8865.
12. Chiang, C. Y.; Hsieh, M. L.; Huang, K. W.; Chau, L. K.; Chang, C. M.; Lyu, S. R., Fiber-optic particle plasmon resonance sensor for detection of interleukin-1beta in synovial fluids. *Biosens Bioelectron* **2010**, *26* (3), 1036-42.
13. Battaglia, T. M.; Masson, J. F.; Sierks, M. R.; Beaudoin, S. P.; Rogers, J.; Foster, K. N.; Holloway, G. A.; Booksh, K. S., Quantification of cytokines involved in wound healing using surface plasmon resonance. *Anal Chem* **2005**, *77* (21), 7016-23.